JOC The Journal of Organic Chemistry

Note

pubs.acs.org/joc

Improved Synthesis of Larger Resorcinarenes

Paolo Della Sala,[†] Carmine Gaeta,*[,†] Wanda Navarra,[†] Carmen Talotta,*[,†] Margherita De Rosa,[†] Giovanna Brancatelli,[‡] Silvano Geremia,[‡] Francesco Capitelli,[§] and Placido Neri[†]

[†]Dipartimento di Chimica e Biologia, Università di Salerno, Via Giovanni Paolo II 132, I-84084 Fisciano (Salerno), Italy

[‡]Centro di Eccellenza in Biocristallografia, Dipartimento di scienze Chimiche e Farmaceutiche, Università di Trieste, via L. Giorgieri 1, 34127 Trieste, Italy

[§]Istituto di Cristallografia-CNR, Via Salaria Km 29.300, 00015 Monterotondo (Roma), Italy

Supporting Information

ABSTRACT: The synthesis of the larger resorcin[5 and 6]arene macrocycles $[5]^{OMe}$ and $[6]^{OMe}$ has been realized by a Lewis acid-catalyzed condensation of 1,3-dimethoxy-2-methylbenzene with paraformaldehyde in *o*-dichlorobenzene as the solvent. The methoxy-resorcin[5 and 6]arenes were quantitatively demethylated by treatment with BBr_3 to obtain the corresponding macrocycles with free OH groups. X-ray studies showed that in the solid state both the conformation and the packing of $[6]^{OMe}$ and $[5]^{OMe}$ are driven by C−H···O, C−H···π, and π···π interactions.

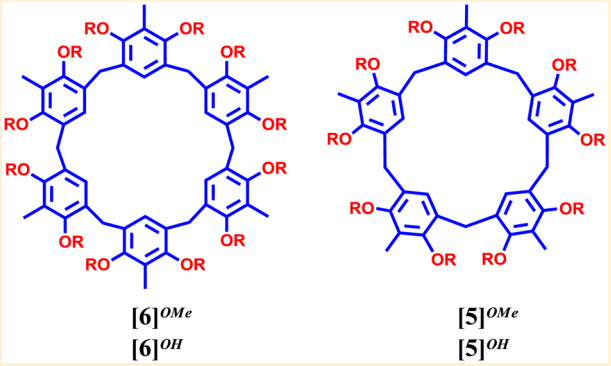

In recent years,[1] the search for novel macrocycles has attracted a considerable amount of attention in view of their potential supramolecular features.[1] These efforts have produced novel classes of hosts such as pillararenes,[2] biphenarenes,[3] calixnaphthalenes,[4] and a wide class of heterocalixarenes,[5] which have found application in several areas of supramolecular chemistry.[6] The success of these macrocycles is largely due to their simple synthesis and purification. In analogy to the most classic calix[*n*]arene[7] macrocycles, they have shown peculiar and size-dependent supramolecular properties.[8]

With regard to the resorcin[*n*]arene macrocycles, a large majority of the work has been devoted to the tetramer (n = 4), which has found many applications as a scaffold for the synthesis of cavitands and self-assembling capsules.[9] In these supramolecular systems, the size of the resorcin[4]arene cavity plays an important role in hosting various guests and selecting them on the basis of their shape and size. Of course, the study of resorcin[*n*]arene macrocycles with more than four resorcinol rings (larger) could pave the way for the synthesis of supramolecular systems with new and intriguing recognition or self-assembly properties.

As opposed to the most popular classes of macrocycles, the chemistry of resorcin[*n*]arenes[9] has been scarcely investigated for the higher homologues (n > 4). In particular, Konishi[10] and co-workers showed that the larger resorcin[6]arene $[6]^{OH}$ (Chart 1) can be obtained by reaction of 2-methylresorcinol with 1,3,5-trioxane in the presence of aqueous concentrated HCl as a catalyst for short reaction times. Interestingly, resorcin[6]arene $[6]^{OH}$ exhibited poor solubility in common organic solvents beacuse of the free OH groups. Therefore, its isolation required the acetylation of the crude reaction mixture followed by purification of the corresponding $[6]^{OAc}$, which was saponified in the presence of KOH to give pure resorcin[6]-arene $[6]^{OH}$.

Chart 1

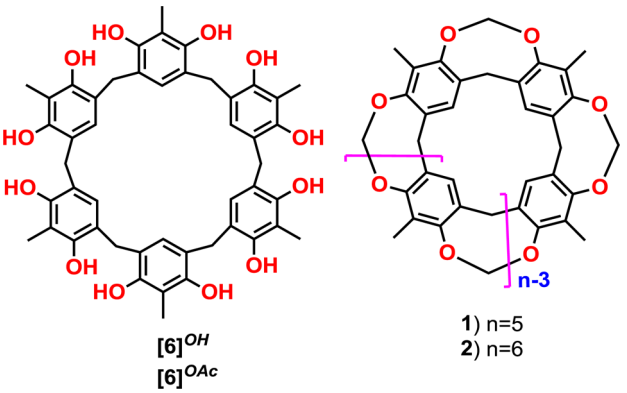

Successively, Sherman[11] and co-workers reported the synthesis of the larger [5,6]cavitands **1** and **2** by treatment of 2-methylresorcinol with diethoxymethane in the presence of aqueous concentrated HCl as a catalyst. In this report, Shermann and co-workers[11] concluded that, "Moreover, it is far easier to purify the cavitand mixture than to isolate the different resorcinarene products and bridge them separately".

Received: April 11, 2016
Published: June 6, 2016

DOI: 10.1021/acs.joc.6b00803
J. Org. Chem. 2016, 81, 5726−5731

Thus, the work of Konishi[10] and Shermann[11] clearly showed that the functionalization of the OH groups of resorcinarene macrocycles strongly improves their solubility in organic solvents, making their workup procedures easier. Prompted by these considerations, we decided to investigate the synthesis of larger resorcin[5,6]arene derivatives by using an O-protected resorcinol substrate, 1,3-dimethoxy-2-methylbenzene **3a**, with the aim of directly obtaining larger resorcinarenes with masked OH functions (Scheme 1), which should improve both purification procedures and synthetic efficiency.

Scheme 1. Lewis Acid-Catalyzed Synthesis of Larger Resorcinarenes[a]

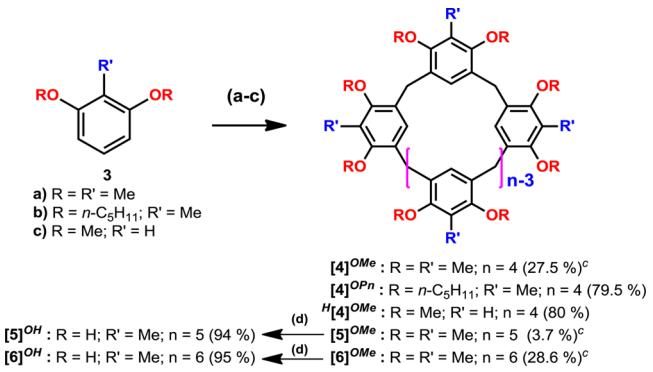

[a]Procedure a: $BF_3{\cdot}Et_2O$, paraformaldehyde, 0.8 M **3a** in dry CH_2ClCH_2Cl, 3 h, 25 °C. Procedure b: $BF_3{\cdot}Et_2O$, paraformaldehyde, 0.6 M **3a** in dry *o*-dichlorobenzene, 4 h, 25 °C. Procedure c: $BF_3{\cdot}Et_2O$, paraformaldehyde, 0.6 M **3a** in *o*-dichlorobenzene, 22 h, 0 °C. Procedure d: BBr_3, dry $CHCl_3$, 298 K, 12 h.

In the first instance, we attempted the condensation of 1,3-dimethoxy-2-methylbenzene **3a** with paraformaldeyde in the presence of a Lewis acid catalyst in accordance with the conditions already reported by Ogoshi[2] for the synthesis of pillararenes. Thus, the treatment of a 0.8 M solution of 1,3-dimethoxy-2- methylbenzene **3a** in CH_2ClCH_2Cl as a solvent and $BF_3{\cdot}Et_2O$ in the presence of paraformaldeyde for 3 h at 25 °C (Scheme 1, procedure a) gave a mixture, which afforded after chromatography resorcin[4]arene-octamethyl ether $[\mathbf{4}]^{OMe}$, resorcin[5]arene-decamethyl ether $[\mathbf{5}]^{OMe}$, and resorcin[6]arene-dodecamethyl ether $[\mathbf{6}]^{OMe}$, in very low yields (25, 5, and 5%, respectively), with a total yield of 35%, in addition to a large quantity of an insoluble polymer.

To improve the yield of large resorcinarenes, we varied the nature of the solvent and focused our attention on *o*-dichlorobenzene. In fact, Chen and co-workers[12] have recently shown that this solvent is effective in the synthesis of large triptycene-based calix[6]arene macrocycle, likely because of a solvent-template effect. Thus, the treatment of a 0.6 M solution of 1,3-dimethoxy-2-methylbenzene **3a** in *o*-dichlorobenzene[12] and $BF_3{\cdot}Et_2O$ in the presence of paraformaldeyde for 4 h at 25 °C (Scheme 1, procedure b) afforded resorcin[4]arene-octamethyl ether $[\mathbf{4}]^{OMe}$, resorcin[5]arene-decamethyl ether $[\mathbf{5}]^{OMe}$, and resorcin[6]arene-dodecamethyl ether $[\mathbf{6}]^{OMe}$ in 60, 8, and 16% yields, respectively, with a total yield of 84%.

In conclusion, using *o*-dichlorobenzene as the solvent and a more diluted condition (0.6 M), we were able to improve the total yield of the reaction from 35 to 84%, to reduce the amount of insoluble material, and to increase the yield of resorcin[6]arene (16%).

Interestingly, Konishi and co-workers previously demonstrated[10b] that the larger resorcin[5]arene and resorcin[6]arene isolated from the reaction of 2-propylresorcinol with formaldehyde in the presence of aqueous concentrated HCl as a catalyst are the kinetically controlled products that can be obtained using shorter reaction times. Unfortunately, the treatment of a 0.6 M solution of 1,3-dimethoxy-2-methylbenzene **3a** in *o*-dichlorobenzene as the solvent and $BF_3{\cdot}Et_2O$ in the presence of paraformaldeyde for 30 or 60 min at 25 °C afforded mainly linear oligomers. Therefore, to favor the kinetically controlled larger macrocycles, we decided to lower the reaction temperature. Thus, when a 0.6 M solution of **3a** was reacted in the presence of paraformaldeyde and $BF_3{\cdot}Et_2O$ at 0 °C for 22 h in *o*-dichlorobenzene (Scheme 1, procedure c), resorcin[6]arene $[\mathbf{6}]^{OMe}$ was isolated in 28.6% yield, while the smaller homologues $[\mathbf{4}]^{OMe}$ and $[\mathbf{5}]^{OMe}$ were obtained in 27.5 and 3.7% yields, respectively. To verify the role of *o*-dichlorobenzene as a templating solvent, we performed the reaction under the same conditions (procedure c, 0 °C) in the presence of 1,2-DCE. The yield of $[\mathbf{6}]^{OMe}$ was lowered to 15%, while $[\mathbf{4}]^{OMe}$ and $[\mathbf{5}]^{OMe}$ were recovered in 22.3 and 1.8% yields, respectively.

With these results in hand (Scheme 1, procedure c), we have varied the nature of the acid and aldehyde to study their influence on the course of the reaction. Thus, the treatment of a 0.6 M solution of **3a** with paraformaldeyde and $SnCl_4$ as the Lewis acid at 0 °C for 22 h in *o*-dichlorobenzene afforded a mixture of $[\mathbf{4}]^{OMe}$, $[\mathbf{5}]^{OMe}$, and $[\mathbf{6}]^{OMe}$ derivatives in which $[\mathbf{4}]^{OMe}$ prevailed (40, 10, and 15%, respectively). Alternatively, the reaction of **3a** with benzaldehyde in the presence of $BF_3{\cdot}Et_2O$ (0 °C for 22 h in *o*-dichlorobenzene) afforded mainly linear oligomers, probably because of the poor reactivity of benzaldehyde at a low temperature.

Compounds $[\mathbf{4}]^{OMe}$, $[\mathbf{5}]^{OMe}$, and $[\mathbf{6}]^{OMe}$ were characterized by spectral analysis. In particular, high- resolution MALDI Fourier transform ion cyclotron resonance mass spectrometry (MALDI-FT-ICR) showed molecular ion peaks at *m*/*z* 679.3263 (Figure S3, calcd *m*/*z* 679.3241), *m*/*z* 843.4077 (Figure S6, calcd *m*/*z* 843.4088), and *m*/*z* 1007.4919 (Figure S9, calcd *m*/*z* 1007.4915), respectively, in accordance with the molecular formulas of $[\mathbf{4}]^{OMe}$ $[M + Na]^+$, $[\mathbf{5}]^{OMe}$ $[M + Na]^+$, and $[\mathbf{6}]^{OMe}$ $[M + Na]^+$, respectively. The ^1H NMR spectrum of resorcin[5]arene-decamethyl ether $[\mathbf{5}]^{OMe}$ in $CDCl_3$ (400 MHz, Figure S4) showed two singlets at 2.19 and 3.56 ppm for the ArCH_3 and OMe groups, respectively. In addition, the presence of a sharp singlet at 3.77 ppm that can be attributed to ArCH_2Ar groups was indicative of the high conformational mobility of the macrocycle, due to the *through-the-annulus passage* of the aromatic rings. Finally, a singlet relative to aromatic protons was present at 6.48 ppm. The ^{13}C NMR spectrum (Figure S5) of pentamer $[\mathbf{5}]^{OMe}$ showed three signals at 9.98, 29.4, and 60.3 ppm for the ArCH_3, ArCH_2Ar, and OCH_3 groups, respectively, while the aromatic carbons were present at 124.2, 129.1, 129.4, and 155.8 ppm. In a similar way, the ^1H NMR spectrum of resorcin[6]arene-dodecamethyl ether $[\mathbf{6}]^{OMe}$ in $CDCl_3$ (600 MHz, Figure S7) showed sharp singlets at 2.15, 3.53, 3.75, and 6.30 ppm for the ArCH_3, OMe, ArCH_2Ar, and ArH hydrogen atoms, respectively. Finally, the ^{13}C NMR spectrum of $[\mathbf{6}]^{OMe}$ (Figure S8) was in accordance with the symmetry of the macrocycle and showed sharp signals at 9.87, 29.6, 60.3, 124.1, 129.0, 129.1, and 155.8 ppm.

When the reaction was repeated starting from 1,3-dipentoxy-2-methylbenzene **3b** bearing longer pentyl chains rather than

DOI: 10.1021/acs.joc.6b00803
J. Org. Chem. 2016, 81, 5726−5731

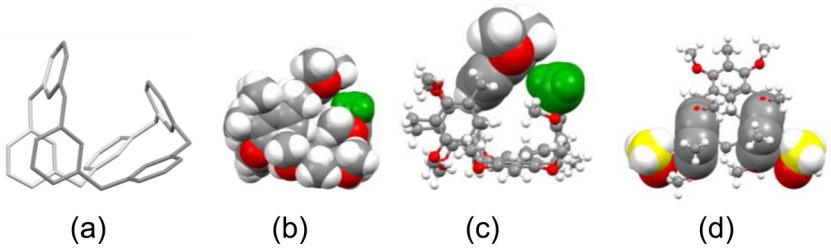

Figure 1. Crystallographic structure of $[\mathbf{6}]^{OMe}$. (a) Folded macrocyclic skeleton (H atoms, ArCH_3, and ArOCH_3 groups have been omitted for the sake of clarity). (b–d) Intramolecular interactions of ArCH_3 (green) and ArOCH_3 (yellow) groups.

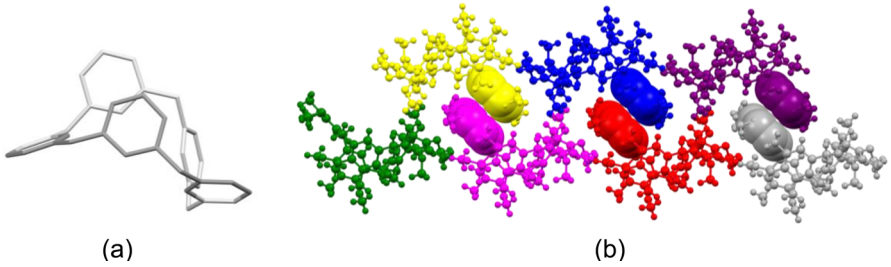

Figure 2. Crystallographic structure of $[\mathbf{5}]^{OMe}$. (a) Hydrogen atoms, methyl groups, and OMe groups have been omitted for the sake of clarity. (b) Packing of $[\mathbf{5}]^{OMe}$ along the *b*-axis.

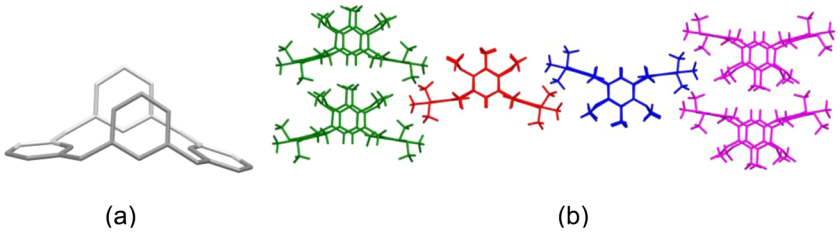

Figure 3. Crystallographic structure of $[\mathbf{4}]^{OMe}$. (a) Hydrogen atoms, methyl groups, and OMe groups have been omitted for the sake of clarity. (b) Packing of $[\mathbf{4}]^{OMe}$ along the *b*-axis.

methyl groups, the resorcin[4]arene $[\mathbf{4}]^{OPn}$ was the only product obtained in 79.5% yield. Analogously, starting from 1,3-dimethoxybenzene **3c** under the same condition, we obtained tetramer $^{H}[\mathbf{4}]^{OMe}$ in 80% yield.[13] The molecular formula of derivative $[\mathbf{4}]^{OPn}$ was confirmed by a ESI(+) mass spectrum that gave a pseudomolecular ion peak $[M + Na]^+$ at m/z 1128.9. Its ^{1}H NMR spectrum in $CDCl_3$ at 298 K showed a triplet at 3.65 ppm, multiplets at 1.69 and 1.36 ppm, and a triplet at 0.90 ppm for the pentyl chains.

The presence of the easily removable methoxy groups in $[\mathbf{5}]^{OMe}$ and $[\mathbf{6}]^{OMe}$ prompted us to attempt their conversion to the corresponding resorcin[5]arene $[\mathbf{5}]^{OH}$ and resorcin[6]arene $[\mathbf{6}]^{OH}$ with free OH groups. Thus, the treatment of $[\mathbf{5}]^{OMe}$ with BBr_3 in dry $CHCl_3$ for 12 h at 25 °C afforded resorcin[5]arene $[\mathbf{5}]^{OH}$ in 94% yield. Analogously, the reaction of $[\mathbf{6}]^{OMe}$ under the same conditions gave resorcin[6]arene $[\mathbf{6}]^{OH}$ in 95% yield. The hydroxy-resorcinarenes $[\mathbf{5}]^{OH}$ and $[\mathbf{6}]^{OH}$ were characterized by spectral analysis. In particular, their HR MALDI-FT-ICR mass spectra showed molecular ion peaks at m/z 703.2519 (Figure S14, calcd m/z 703.2513) and 839.3053 (Figure S17, calcd m/z 839.3043) in accordance with the molecular formulas of $[\mathbf{5}]^{OH}$ and $[\mathbf{6}]^{OH}$, respectively. The ^{1}H NMR spectra of $[\mathbf{5}]^{OH}$ and $[\mathbf{6}]^{OH}$ in acetone-d_6 (400 MHz) showed OH singlets at 7.76 and 8.09 ppm, respectively. Like $[\mathbf{6}]^{OMe}$, the corresponding demethylated analogue $[\mathbf{6}]^{OH}$ showed a sharp ArCH_2Ar singlet at 3.74 ppm (^{1}H NMR in acetone-d_6, 400 MHz) indicative of the high conformational mobility of the macrocycle. No hint of coalescence of the ArCH_2Ar singlet of $[\mathbf{6}]^{OH}$ was observed when the temperature was decreased to 215 K.

Interestingly, X-ray studies showed that in the solid state resorcin[6]arene $[\mathbf{6}]^{OMe}$ adopts a folded (Figure 1a,b) conformation driven by weak intramolecular interactions. A fundamental one is the Ar$\mathbf{C}$H$_2$–H$\cdots\pi^{centroid}$ interaction (methyl fragment and aryl group colored green and gray, respectively, in Figure 1b,c) with a Ph–H$_3\mathbf{C}\cdots\pi^{centroid}$ distance of 4.22 Å. In addition, two O$\mathbf{CH_2}$–H$\cdots\pi$ interactions are present between two OCH$_3$ groups (yellow in Figure 1d) and two aromatic rings (Figure 1d), with $\mathbf{C}$H$_2$–H$\cdots\pi$ distances of 3.67 and 4.17 Å. Interestingly, two weak $\mathbf{C}$–H$\cdots\mathbf{O}$ hydrogen bonding interactions[14] were evidenced (Figure S18a) with distances of 3.62 and 3.59 Å and C–H$\cdots$O angles of 161.9(1)° and 165.6(1)°, respectively. In a similar way, the packing of $[\mathbf{6}]^{OMe}$ is also stabilized by weak $\mathbf{C}$–H$\cdots\mathbf{O}$ hydrogen bonds[14] (Figure S18a) in addition to $\pi\cdots\pi$ interactions, with an average distance between aromatic baricenters of 3.70 Å (Figure S18b).

Analogous X-ray studies showed that in the solid state cyclopentamer $[\mathbf{5}]^{OMe}$ adopts a distorted structure, resembling the flattened saddle[15] conformation (Figure 2a), to ensure the packing through intermolecular contacts (Figure 2). Thus, along the *b*-axis, the $[\mathbf{5}]^{OMe}$ molecule established $\pi\cdots\pi$ interactions with an average distance between the aromatic baricenters of 3.52 Å. In addition, the stacked aromatic rings (Figure 2) estabilished four CH$\cdots$O weak hydrogen bonds

DOI: 10.1021/acs.joc.6b00803
J. Org. Chem. 2016, 81, 5726–5731

between the $ArCH_2Ar$ and OCH_3 groups, with an average distance of 3.38 Å and an average $HC-H\cdots OCH_3$ bond angle of 136.6°.

The smaller resorcin[4]arene $[\mathbf{4}]^{OMe}$ homologue showed in the solid state a boat[13b,c] structure in which two distal aromatic rings are perpendicular to the mean plane of the $ArCH_2Ar$ groups, while the other two are almost coplanar to it (Figure 3a).

In analogy to the higher homologues, also for $[\mathbf{4}]^{OMe}$ weak H-bonding[14] interactions are effective in the stabilization of the solid-state assembly. Thus, molecules of $[\mathbf{4}]^{OMe}$ are linked by weak intermolecular H-bonds, which stabilize the antiparallel columnar assemblies running along the *c*-axis (green−red−green and magenta−blu−magenta in Figure 3b). Interstingly, along the *b*-axis, $[\mathbf{4}]^{OMe}$ units (red and blue in Figure 3b and Figure S19), which have opposite orientations, are assembled through $ArCH_2-H\cdots\pi$ interaction (Figure S19) with a $C-H\cdots\pi^{centroid}$ distance of 3.46 Å.

With regard to the conformation adopted by the larger $[\mathbf{6}]^{OMe}$ resorcinarene in solution, molecular mechanics calculations[16] (Monte Carlo conformational search, 10000 steps, MacroModel version 9.0, MM3 force field, $CHCl_3$ solvent, GB/SA model) (Figure S24) indicated the folded structure found in the solid state (Figure 1a) as the lowest-MM3 energy conformation (Figure S24). The high degree of similarity between the lowest MM3 energy conformation (Figure 3a) and the X-ray structure of $[\mathbf{6}]^{OMe}$ (Figure S24) was confirmed by a root-mean-square deviation (rmsd) of 0.70 Å for their superimposition (Figure S24). Analogously, for the $[\mathbf{5}]^{OMe}$ derivative, molecular mechanics calculations indicated the distorted flattened saddle structure in Figure 2a as the lowest-MM3 energy conformation (Figure S23; rmsd = 1.01 Å). Derivatives $[\mathbf{5}]^{OMe}$ and $[\mathbf{6}]^{OMe}$ exhibit a very fast conformational mobility as demonstrated by ^1H VT NMR studies (Figure S25), which have shown no hint of coalescence for their sharp ^1H NMR signals down to 230 K.

In conclusion, we here have introduced a new and more efficient procedure for the synthesis of the larger resorcin[5 and 6]arene macrocycles by a BF_3-catalyzed condensation of 1,3-dimethoxy-2-methylbenzene with paraformaldehyde in *o*-dichlorobenzene as the solvent at 0 °C. The obtained methoxy-resorcin[5 and 6]arenes have been quantitatively demethylated by treatment with BBr_3 to produce the corresponding derivatives with free OH groups. X-ray studies showed that in the solid state both the conformation and the packing of methoxy-resorcin[5 and 6]arenes are driven by weak $C-H\cdots O$, $C-H\cdots\pi$, and $\pi\cdots\pi$ interactions. The larger resorcinarene macrocycles described here can be considered useful scaffolds for obtaining resorcinarene-based hosts and cavitands with novel and intruiguing supramolecular properties.

EXPERIMENTAL SECTION

General Information. HR MALDI mass spectra were recorded on a FT-ICR mass spectrometer equipped with a 7T magnet. The samples were ionized in positive ion mode using the MALDI ion source, and 15 laser shots were used for each scan. The mass spectra were calibrated externally, and a linear calibration was applied. To improve the mass accuracy, the spectra were recalibrated internally by matrix ionization (2,5-DHB). Samples were prepared by mixing 10 μL of analyte in dichloromethane (1 mg/mL) with 10 μL of a saturated (30 mg/mL) solution of 2,5-DHB. ESI(+)-MS measurements were performed on a triple-quadrupole mass spectrometer equipped with an electrospray ion source, using $CHCl_3$ as the solvent. All chemicals were reagent grade and used without further purification. Anhydrous solvents were used as purchased from the supplier. When necessary, compounds were dried *in vacuo* over $CaCl_2$. Reaction temperatures were measured externally. Reactions were monitored by TLC silica gel plates (0.25 mm) and visualized by UV light, or by spraying with $H_2SO_4-Ce(SO_4)_2$. NMR spectra were recorded on a 600 [600 (^1H) and 150 MHz (^{13}C)], 400 MHz [400 (^1H) and 100 MHz (^{13}C)], or 300 MHz [300 (^1H) and 75 MHz (^{13}C)] spectrometer. Chemical shifts are reported relative to the residual solvent peak.

Crystallographic Determination of Compounds $[\mathbf{4}]^{OMe}$, $[\mathbf{5}]^{OMe}$, and $[\mathbf{6}]^{OMe}$. Small single crystals of compounds $[\mathbf{5}]^{OMe}$ and $[\mathbf{6}]^{OMe}$ were obtained by slow evaporation of a methanol/chloroform solution and analyzed by synchrotron X-ray diffraction analysis. Routinely a crystal dipped in Paratone, as cryoprotectant, is mounted on a loop and immediately flash-frozen under a liquid nitrogen stream at a 100 K. Diffraction images of compounds $[\mathbf{5}]^{OMe}$ and $[\mathbf{6}]^{OMe}$ were integrated by using XDS[17] and MOSFLM,[18] respectively. Data sets were then scaled by using XSCALE[19] and SCALA[20] compounds $[\mathbf{5}]^{OMe}$ and $[\mathbf{6}]^{OMe}$. The crystal structures were determined by Direct Methods with the SIR2014[21] software and refined with SHELX-13.[22] Thermal parameters of all non-hydrogen atoms were refined anisotropically, and hydrogen atoms were placed at the geometrically calculated positions and refined using the riding model. Crystallographic data and refinement details are reported in Table S1. Crystals of $[\mathbf{4}]^{OMe}$ were obtained by slow evaporation of a methanol/chloroform solution and collected on a Nonius KappaCCD diffractometer, equipped with graphite-monochromated Mo Kα radiation (λ = 0.71073 Å). The structure was determined (Table S1) through the Direct Methods procedure of SIR2008.[23] Refinement of the crystal structures was conducted via a full-matrix least-squares technique based on F^2, SHELXL-97;[24] the non-hydrogen atoms were refined with anisotropic thermal parameters, while the hydrogen atoms were placed in idealized positions riding on their attached atoms [$C-H_{Ar}$, 0.93 Å; $C-H_{Methyl}$, 0.96 Å; $C-H_{Methylene}$, 0.97 Å; $U_{iso}(H)_{Ar/Methylene}$, $1.2U_{iso}(C)$; $U_{iso}(H)_{Methyl}$, $1.5U_{iso}(C)$].

Synthesis of Resorcinarenes $[\mathbf{4}-\mathbf{6}]^{OMe}$. *Procedure b.* A suspension of 1,3-dimethoxy-2-methylbenzene (1.00 g, 6.57 mmol) and paraformaldehyde (0.24 g, 7.88 mmol) in dry 1,2-dichlorobenzene (11 mL) was degassed for 30 min.

Then the reaction mixture was cooled to 0 °C, and $BF_3\cdot OEt_2$ (0.97 mL, 7.88 mmol) was added and the mixture stirred for 4 h at 25 °C under a nitrogen atmosphere. The solvent was evaporated, and the solid was dissolved in ethyl acetate (100 mL) and washed with H_2O (2 × 100 mL). The organic phase was extracted, dried with Na_2SO_4, and evaporated to obtain a white solid. The crude product was dissolved in 10 mL of a 2:8 (v/v) hexane/CH_2Cl_2 solvent and purified by column chromatography on silica gel (60 g) using a hexane/CH_2Cl_2/ethyl acetate gradient (from 80:14:6 to 80:3:17). Derivative $[\mathbf{4}]^{OMe}$: white solid; 0.65 g, 60% yield; mp 234−235 °C; ^1H NMR (400 MHz, $CDCl_3$, 298 K) δ 6.19 (s, 4H), 3.82 (s, 8H), 3.63 (s, 24H), 2.21 (s, 12H); ^{13}C NMR (100 MHz, $CDCl_3$, 298 K) δ 155.9, 129.1, 128.9, 123.8, 60.4, 29.4, 9.88; HRMS (MALDI) m/z $[M + Na]^+$ calcd for $C_{40}H_{48}NaO_8$ 679.3241, found 679.3263. Derivative $[\mathbf{5}]^{OMe}$: white solid; 0.086 g, 8.0% yield; mp 161−162 °C; ^1H NMR ($CDCl_3$, 400 MHz, 298 K) δ 6.48 (s, 5H), 3.77 (s, 10H), 3.56 (s, 30H), 2.19 (s, 15H); ^{13}C NMR ($CDCl_3$, 100 MHz, 298 K) δ 155.8, 129.4, 129.1, 124.2, 60.3, 29.4, 9.98; HRMS (MALDI) m/z $[M + Na]^+$ calcd for $C_{50}H_{60}NaO_{10}$ 843.4088, found 843.4077. Derivative $[\mathbf{6}]^{OMe}$: white solid; 0.17 g, 16% yield; mp 222−223 °C; ^1H NMR ($CDCl_3$, 600 MHz, 298 K) δ 6.30 (s, 6H), 3.75 (s, 12H), 3.53 (s, 36H), 2.15 (s, 18H); ^{13}C NMR ($CDCl_3$, 75 MHz, 298 K) δ 155.8, 129.1, 129.0, 124,1, 60.3, 29.6, 9.87; HRMS (MALDI) m/z $[M + Na]^+$ calcd for $C_{60}H_{72}NaO_{12}$ 1007.4915, found 1007.4919.

Procedure c. A suspension of 1,3-dimethoxy-2-methylbenzene (0.50 g, 3.28 mmol) and paraformaldehyde (0.12 g, 3.94 mmol) in dry 1,2-dichlorobenzene (5.5 mL) was degassed for 30 min. Then the reaction mixture was cooled to 0 °C, and $BF_3\cdot OEt_2$ (0.48 mL, 3.94 mmol) was added and the mixture stirred for 22 h at 0 °C under a nitrogen atmosphere. The solvent was evaporated, and the solid was dissolved in ethyl acetate (50 mL) and washed with H_2O (2 × 50 mL). The organic phase was extracted, dried with Na_2SO_4, and evaporated to

DOI: 10.1021/acs.joc.6b00803
J. Org. Chem. 2016, 81, 5726−5731

obtain a white solid. The crude product was dissolved in 5 mL of a 2:8 (v/v) hexane/CH_2Cl_2 solvent and purified by column chromatography on silica gel (30 g) using a hexane/CH_2Cl_2/ethyl acetate gradient (from 80:14:6 to 80:3:17). Derivative $[4]^{OMe}$: white solid; 0.147 g, 27.5% yield. Derivative $[5]^{OMe}$: white solid; 0.02 g, 3.7% yield. Derivative $[6]^{OMe}$: white solid; 0.154 g, 28.6% yield.

Synthesis of Resorcinarenes $[4-6]^{OH}$. *General Procedure.* To a solution of appropriate resorcinarene $[4-6]^{OMe}$ (0.36 mmol) in dry $CHCl_3$ (18 mL) under a nitrogen atmosphere was added BBr_3 (0.53 mL, 5.50 mmol), and the mixture was stirred at room temperature. After 12 h, the reaction mixture was evaporated and the crude material was dissolved in ethyl acetate and washed two times with a saturated solution of Na_2SO_3 (50 mL). The organic phase was extracted and washed with H_2O (50 mL), and the solvent was removed under reduced pressure.

Derivative $[5]^{OH}$: 0.23 g, 94% yield; mp >257 °C dec; ^{1}H NMR (acetone-d_6, 250 MHz, 298 K) δ 7.76 (s), 6.81 (s, 5H), 3.68 (s, 10H), 2.12 (s, 15H); ^{13}C NMR (acetone-d_6, 75 MHz, 298 K) δ 151.8, 129.5, 120.5, 112.4, 31.4, 9.56; HRMS (MALDI) m/z $[M + Na]^+$ calcd for $C_{40}H_{40}NaO_{10}$ 703.2513, found 703.2519.

Derivative $[6]^{OH}$: 0.28 g, 95% yield; mp >230 °C dec; ^{1}H NMR (acetone-d_6, 250 MHz, 298 K) δ 8.09 (s), 7.43 (s, 6H), 3.74 (s, 12H), 2.10 (s, 18H); ^{13}C NMR (acetone-d_6, 75 MHz, 298 K) δ 151.0, 129.5, 122.1, 112.8, 31.3, 9.62; HRMS (MALDI) m/z $[M + Na]^+$ calcd for $C_{48}H_{48}NaO_{12}$ 839.3043, found 839.3053.[25]

Synthesis of $[4]^{OPn}$. A suspension of 1,3-dipentoxy-2-methylbenzene **3b** (1.50 g, 5.67 mmol) and paraformaldehyde (0.18 g, 5.67 mmol) in dry 1,2-dichloroethane (9.5 mL) was degassed for 30 min. After this step, the reaction mixture was cooled to 0 °C and $BF_3{\cdot}OEt_2$ (0.97 mL, 7.88 mmol) was added and the mixture stirred for 3 h at 25 °C under a nitrogen atmosphere. Then, the solvent was evaporated and the solid crude product dissolved in ethyl acetate (100 mL) and washed with H_2O (100 mL). The organic phase was extracted, dried with Na_2SO_4, and evaporated to obtain crude material that was triturated with MeOH (20 mL) to give derivative $[4]^{OPn}$: white solid; 1.24 g, 79.5% yield; mp >260 °C dec; ESI(+)-MS m/z 1128.9 ($M + Na^+$); ^{1}H NMR ($CDCl_3$, 400 MHz, 298 K) δ 6.17 (s, 4H), 3.81 (s, 8H), 3.65 (t, 16H), 2.18 (s, 12H), 1.69 (m, 16H), 1.36 (m, 32H), 0.90 (t, 32H); ^{13}C NMR ($CDCl_3$, 63 MHz, 298 K) δ 155.0, 128.9, 123.8, 72.9, 30.4, 29.6, 28.5, 22.8, 14.2, 10.2. Anal. Calcd for $C_{72}H_{112}O_8$: C, 78.21; H, 10.21. Found: C, 78.31; H, 10.13.

■ ASSOCIATED CONTENT

Supporting Information

The Supporting Information is available free of charge on the ACS Publications website at DOI: 10.1021/acs.joc.6b00803.

1D ^{1}H and ^{13}C NMR spectra, HR mass spectra, X-ray figures, and a table of crystal data for $[4]^{OMe}$, $[5]^{OMe}$, and $[6]^{OMe}$ (PDF)

Crystallographic data for $[4]^{OMe}$ (CIF)

Crystallographic data for $[5]^{OMe}$ (CIF)

Crystallographic data for $[6]^{OMe}$ (CIF)

■ AUTHOR INFORMATION

Corresponding Authors

*E-mail: cgaeta@unisa.it.

*E-mail: ctalotta@unisa.it.

Notes

The authors declare no competing financial interest.

■ ACKNOWLEDGMENTS

We thank the Italian MIUR (PRIN 20109Z2XRJ_006) for financial support and the Centro di Tecnologie Integrate per la Salute (Project PONa3_00138), Università di Salerno, for the 600 MHz NMR instrumental time. Thanks are due to Dr. Patrizia Oliva and Dr. Patrizia Iannece for instrumental assistance.

■ REFERENCES

(1) Neri, P., Sessler, J. L., Wang, M.-X., Eds. *Calixarenes and Beyond*; Springer: Dordrecht, The Netherlands, 2016.

(2) Ogoshi, T.; Kanai, S.; Fujinami, S.; Yamagishi, T.; Nakamoto, Y. *J. Am. Chem. Soc.* **2008**, *130*, 5022−5023.

(3) Chen, H.; Fan, J.; Hu, X.; Ma, J.; Wang, S.; Li, J.; Yu, Y.; Jia, X.; Li, C. *Chem. Sci.* **2015**, *6*, 197−202.

(4) Georghiou, P. E.; Li, Z.; Ashram, M.; Chowdhury, S.; Mizyed, S.; Tran, A. H.; Al-Saraierh, H.; Miller, D. O. *Synlett* **2005**, 879−891.

(5) Wang, M.−X.; Zhang, X.−H.; Zheng, Q.−Y. *Angew. Chem., Int. Ed.* **2004**, *43*, 838−843.

(6) (a) Ogoshi, T.; Takashima, S.; Yamagishi, T.-a. *J. Am. Chem. Soc.* **2015**, *137*, 10962−10964. (b) Wang, M.−X. *Acc. Chem. Res.* **2012**, *45*, 182−195.

(7) (a) Gutsche, C. D. *Calixarenes, an Introduction*; Royal Society of Chemistry: Cambridge, U.K., 2008. (b) Asfari, Z., Böhmer, V., Harrowfield, J., Vicens, J., Eds. *Calixarenes 2001*; Kluwer: Dordrecht, The Netherlands, 2001. (c) Vicens, J., Harrowfield, J., Eds. *Calixarenes in the Nanoworld*; Springer: Dordrecht, The Netherlands, 2007.

(8) (a) Bandela, A. K.; Bandaru, S.; Rao, C. P. *Chem. - Eur. J.* **2015**, *21*, 13364−13374. (b) Troisi, F.; Russo, A.; Gaeta, C.; Bifulco, G.; Neri, P. *Tetrahedron Lett.* **2007**, *48*, 7986−7989. (c) Talotta, C.; Gaeta, C.; Neri, P. *Org. Lett.* **2012**, *14*, 3104−3107. (d) Recently, a review of the synthesis of oxacalix[3]arenes has been reported. See: Cottet, K.; Marcos, P. M.; Cragg, P. J. *Beilstein J. Org. Chem.* **2012**, *8*, 201−226 and references cited therein..

(9) (a) Cram, D. J.; Cram, J. M. In *Container Molecules and Their Guests*; Monographs in Supramolecular Chemistry; Stoddart, J. F., Ed.; Royal Society of Chemistry: Cambridge, U.K., 1994. (b) Ajami, D.; Liu, L.; Rebek, J., Jr. *Chem. Soc. Rev.* **2015**, *44*, 490−499. (c) MacGillivray, L. R.; Atwood, J. L. *Nature* **1997**, *389*, 469−472.

(10) (a) Konishi, H.; Ohata, K.; Morikawa, O.; Kobayashi, K. *J. Chem. Soc., Chem. Commun.* **1995**, 309−310. (b) Konishi, H.; Nakamura, T.; Ohata, K.; Kobayashi, K.; Morikawa, O. *Tetrahedron Lett.* **1996**, *37*, 7383−7386.

(11) Naumann, C.; Román, E.; Peinador, C.; Ren, T.; Patrick, B. O.; Kaifer, A. E.; Sherman, J. C. *Chem. - Eur. J.* **2001**, *7*, 1637−1645.

(12) Tian, X.-H.; Hao, X.; Liang, T.-L.; Chen, C.-F. *Chem. Commun.* **2009**, 6771−6773.

(13) (a) Falana, O. M.; Al-Farhan, E.; Keehn, P. M.; Stevenson, R. *Tetrahedron Lett.* **1994**, *35*, 65−68. (b) Morikawa, O.; Ishizaka, T.; Sakakibara, H.; Kobayashi, K.; Konishi, H. *Polym. Bull.* **2005**, *53*, 97−107. (c) Li, D.; Suzuki, T.; Konishi, H.; Yamagishi, T.-A.; Nakamoto, Y. *Polym. Bull.* **2002**, *48*, 423−429.

(14) Steiner, T. *Angew. Chem., Int. Ed.* **2002**, *41*, 48−76.

(15) A solid-state flattened saddle structure has been observed for NH-bridged calix[2]arene[2] pyridine: Yao, B.; Wang, D.-X.; Gong, H.-Y.; Huang, Z.-T.; Wang, M.-X. *J. Org. Chem.* **2009**, *74*, 5361−5368.

(16) Molecular modeling was performed with MacroModel, version 9.0, Schrödinger, LLC, New York, 2005: Mohamadi, F.; Richards, N. G.; Guida, W. C.; Liskamp, R.; Lipton, M.; Caufield, C.; Chang, G.; Hendrickson, T.; Still, W. C. *J. Comput. Chem.* **1990**, *11*, 440−467.

(17) Kabsch, W. *Acta Crystallogr., Sect. D: Biol. Crystallogr.* **2010**, *66*, 125−132.

(18) Battye, G. G.; Kontogiannis, L.; Johnson, O.; Powell, H. R.; Leslie, A. G. W. *Acta Crystallogr., Sect. D: Biol. Crystallogr.* **2011**, *67*, 271−281.

(19) Kabsch, W. *Acta Crystallogr., Sect. D: Biol. Crystallogr.* **2010**, *66*, 133−144.

(20) (a) Evans, P. R. *Acta Crystallogr., Sect. D: Biol. Crystallogr.* **2006**, *62*, 72−82. (b) Winn, M. D.; Ballard, C. C.; Cowtan, K. D.; Dodson, E. J.; Emsley, P.; Evans, P. R.; Keegan, R. M.; Krissinel, E. B.; Leslie, A. G. W.; McCoy, A.; McNicholas, S. J.; Murshudov, G. N.; Pannu, N. S.; Potterton, E. A.; Powell, H. R.; Read, R. J.; Vagin, A.; Wilson, K. S. *Acta Crystallogr., Sect. D: Biol. Crystallogr.* **2011**, *67*, 235−242.

DOI: 10.1021/acs.joc.6b00803
J. Org. Chem. 2016, 81, 5726−5731

(21) Burla, M. C.; Caliandro, R.; Carrozzini, B.; Cascarano, G. L.; Cuocci, C.; Giacovazzo, C.; Mallamo, M.; Mazzone, A.; Polidori, G. *J. Appl. Crystallogr.* **2015**, *48*, 306−309.
(22) Sheldrick, G. M. *Acta Crystallogr., Sect. A: Found. Crystallogr.* **2008**, *64*, 112−122.
(23) Burla, M. C.; Caliandro, R.; Camalli, M.; Carrozzini, B.; Cascarano, G. L.; De Caro, L.; Giacovazzo, C.; Polidori, G.; Siliqi, D.; Spagna, R. *J. Appl. Crystallogr.* **2007**, *40*, 609−613.
(24) Sheldrick, G. M. *SHELXL-97. Program for the Refinement of Crystal Structures*; University of Gottingen: Gottingen, Germany, 1997.
(25) ^{1}H and ^{13}C NMR spectra reported by Konishi and co-workers in ref 10a were obtained at 50 °C in $(CD_3)_2SO_4$: ^{1}H NMR (270 MHz) δ 2.037 (s, 18H, CH_3), 3.605 (s, 12H, bridge CH_2), 6.990 (s, 6H, aromatic), 8.51 (s, 12H, OH); ^{13}C NMR (67.5 MHz) δ 69.7, 30.2, 112.2, 120.6, 127.8, 150.1. For a recent report on the X-ray structure of the $[\mathbf{6}]^{OH}$ derivative, see: Brancatelli, G.; Geremia, S.; Gaeta, C.; Della Sala, P.; Talotta, C.; De Rosa, M.; Neri, P. *CrystEngComm* **2016**, DOI: 10.1039/C6CE00802J.

DOI: 10.1021/acs.joc.6b00803
J. Org. Chem. 2016, 81, 5726−5731